Ament Model for Multiple Rebounds From Rough Sea Surfaces in a Stratified Medium and Validation From the MoM-Based Multilevel SDIM

Dušan Cvetković, Christophe Bourlier, and Nicolas Pinel

***Abstract*— In this paper, the well-known Ament model is generalized to multiple rebounds (reflections) from rough sea surfaces in a stratified medium. To solve this propagation-scattering problem in the radar microwave domain, the physical optics (PO) approximation is applied to determine the currents on the rough sea surface. Next, to solve the propagation problem, i.e., to calculate the scattered field in the duct, an appropriate Green function of the duct (which is a stratified medium with linear-square refraction index profile) is used to radiate the currents from Huygens' principle. Due to refraction phenomenon, this field induces new currents on the surface (second rebound), which are again evaluated by PO. The process is iterated. Then, for each rebound, the coherent components of the surface currents and the scattered field are calculated and compared with those of a flat surface in order to derive the generalized Ament model. In addition, this model is compared with the results computed by the rigorous method of moments and accelerated by the multilevel subdomain decomposition iterative method combined with the adaptive cross approximation.**

***Index Terms*— Green function, method of moments (MoM), physical optics (PO) approximation, rough surface scattering, sea surface, stratified media.**

I. Introduction

SINCE the mid-twentieth century, electromagnetic modeling in the marine environment at low-grazing angles has been an important issue in the scientific research. In order to determine the electromagnetic field above the sea surface, two main problems must be solved: the wave scattering caused by the surface roughness and the propagation within a duct existing above the surface. This duct represents a medium made up of small layers due to the atmospheric inhomogeneities. Furthermore, the scattering effect is especially important for the electromagnetic waves with a low-grazing incidence, occurring at coastal radar configurations. Therefore, various models have been developed to account for these phenomena.

The first well-known model handling the surface scattering was established in [1]. It is a simple and fast asymptotic model based on a ray approach, and it assumes a homogeneous medium of propagation. It considers the radar propagation in the specular direction over the rough surface, and it is frequently employed for determining the coherent scattered field. Notably, the most commonly applied electromagnetic wave propagation method based on the parabolic wave equation (PWE) [2] uses the Ament approximation to include the sea surface roughness. Later, Miller *et al.* [3] and Freund *et al.* [4] have presented a modification of the Ament model, which showed better agreement with experimental measurements for stronger sea roughness. However, this result was re-examined by Hristov *et al.* [5], who concluded that the fundamental assumptions on the sea surface statistics used by Ament are physically more justified. Finally, the Ament model can be improved by introducing the shadowing effect [6]–[8].

In this paper, we derive the generalized Ament model to multiple rebounds (reflections) by a rough sea surface in a stratified medium. To solve this propagation-scattering problem, the physical optics (PO) approximation is applied to determine the currents on the rough sea surface. Next, to solve the propagation problem, i.e., to calculate the scattered field in the duct, an appropriate Green function of the duct (which is a stratified medium with linear-square refraction index profile) is used to radiate the currents from Huygens' principle. Its calculation is based on the PWE approximation. After, for each rebound, the coherent components of the surface currents and the scattered field are calculated and compared with those of a flat surface in order to derive the generalized Ament model. Thus, this coefficient is obtained for the first time for multiple rebounds and in duct conditions. Furthermore, this rapid model avoids the application of the time-consuming Monte Carlo process in order to obtain the coherent component. This result is solved for a perfectly conducting (PC) surface, but can be extended for a highly conducting surface if the impedance boundary condition is applied. In addition, this model is compared with the results computed by the rigorous method of moments (MoM) and accelerated by the multilevel subdomain decomposition iterative method (SDIM) combined with the adaptive cross approximation (ACA) [9].

This paper is organized as follows. In Section II, the theoretical model is presented, and Sections III and IV present the derivation of the components of the surface currents and scattered field by introducing the generalized Ament model. Section V shows the numerical results, and Section VI gives concluding remarks.

II. Theoretical Model

Let us consider a 2-D space $\Omega = \Omega_1 \cup \Omega_2 \cup \Omega_3$ (see Fig. 1) made up of a homogeneous medium Ω_1 (defined for $z \geq h$)

Manuscript received May 12, 2015; revised December 10, 2015; accepted March 29, 2016. Date of publication May 10, 2016; date of current version July 5, 2016.

D. Cvetković and C. Bourlier are with the Institut d'Electronique et de Télécommunications de Rennes Laboratory, LUNAM Université, Université de Nantes, La Chantrerie, BP 50609, Nantes 44306, France (e-mail: dusan.cvetkovic@etu.univ-nantes.fr; christophe.bourlier@univ-nantes.fr).

N. Pinel is with Alyotech, Rennes 35700, France (e-mail: nicolas.pinel@univ-nantes.fr).

Color versions of one or more of the figures in this paper are available online at http://ieeexplore.ieee.org.

Digital Object Identifier 10.1109/TAP.2016.2565678

0018-926X © 2016 IEEE. Personal use is permitted, but republication/redistribution requires IEEE permission.
See http://www.ieee.org/publications_standards/publications/rights/index.html for more information.

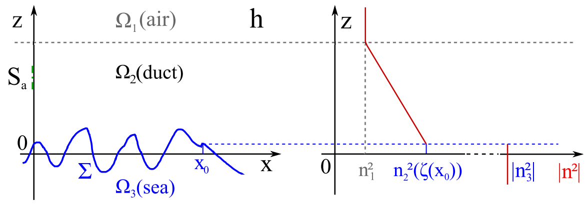

Fig. 1. Left: illustration of the scattering problem. Right: profile of the modulus of the square of the refractive index.

with a constant refractive index n_1 above an inhomogeneous medium $\mathbf{\Omega}_2$ [defined for $\zeta(x) \leq z < h$], which represents a duct with a linear-square refractive index profile, defined by $n^2(z) = n_1^2 + \varepsilon(h - z)$, $\zeta(x) \leq z < h$, with $\varepsilon > 0$. $h > 0$ denotes the duct height. Furthermore, media $\mathbf{\Omega}_2$ and $\mathbf{\Omega}_3$ are separated by a rough sea surface Σ of altitude $\zeta(x)$, in which x is its abscissa. In media $\mathbf{\Omega}_1$ and $\mathbf{\Omega}_2$, the refractive indices are positive real numbers and the refractive index in $\mathbf{\Omega}_3$, n_3, is a constant complex number with a large imaginary part in comparison with unity at the frequencies of interest. Thereby, we can consider the sea surface to be PC.

In reality, the medium $\mathbf{\Omega}_1$, generally, also has a negative gradient of the refraction index. In our case, we are interested in propagation inside the duct, and therefore the incidence angle and the height of the transmitter are chosen to have the field almost completely inside the duct. Considering the medium $\mathbf{\Omega}_1$ homogeneous does not influence the results.

A. Surface Currents and Scattered Field

In order to calculate the scattered field in the duct, it is necessary to know the currents on the 1-D surface [10]. In 2-D space, the currents, denoted by $\{\psi(\boldsymbol{r}), \partial_n \psi(\boldsymbol{r})\}$, can be determined by solving the integral equations from an MoM [11]. Another way to calculate the surface currents is to apply the PO approximation, which is expected to work well for scattered fields around the so-called specular direction. This leads $\forall \boldsymbol{r} \in \Sigma$ to [12]

$$\begin{cases} \psi^{(1)}(\boldsymbol{r}) = [1 + \mathcal{R}(\chi_1)]\psi_{\text{inc}}(\boldsymbol{r}) \\ \partial_n \psi^{(1)}(\boldsymbol{r}) = [1 - \mathcal{R}(\chi_1)]\partial_n \psi_{\text{inc}}(\boldsymbol{r}) \end{cases} \tag{1}$$

where the superscript (1) stands for the currents corresponding to the first bound on the surface. In addition, $\partial_n = \partial/\partial n = (-\gamma\, \partial_x + \partial_z)$ is the normal derivative operator on the surface, in which the surface slope is $\gamma = \partial_x \zeta$. Moreover, ψ_{inc} is the incident field on the surface and $\boldsymbol{r} = x\hat{\boldsymbol{x}} + z\hat{\boldsymbol{z}}$ is a vector of components (x, z) in the Cartesian basis $(\hat{\boldsymbol{x}}, \hat{\boldsymbol{z}})$. Finally, $\mathcal{R}$ is the Fresnel reflection coefficient in either vertical (TM) or horizontal (TE) polarization. In general, it depends on the local incidence angle χ_1 at the interface.

Thus, knowing the currents on the surface $\{\psi(\boldsymbol{r}), \partial_n \psi(\boldsymbol{r})\}$, the scattered field in $\mathbf{\Omega}_2$ can be computed by applying Huygens' principle, leading $\forall \boldsymbol{r}' \in \mathbf{\Omega}_2$ to

$$\psi_{\text{sca}}(\boldsymbol{r}') = \int_x [\psi(\boldsymbol{r})\partial_n g(\boldsymbol{r}, \boldsymbol{r}') - g(\boldsymbol{r}, \boldsymbol{r}')\partial_n \psi(\boldsymbol{r})]dx \tag{2}$$

where g is the spatial Green function in $\mathbf{\Omega}_2$.

Then, the field scattered from the surface of the first order is $\forall \boldsymbol{r}'_1 \in \mathbf{\Omega}_2$

$$\psi_{\text{sca}}^{(1)}(\boldsymbol{r}') = \int_x \big[\mathcal{R}_+(\chi_1)\psi_{\text{inc}}^{(1)}(\boldsymbol{r})\partial_n g(\boldsymbol{r}, \boldsymbol{r}') - \mathcal{R}_-(\chi_1)g(\boldsymbol{r}, \boldsymbol{r}')\partial_n \psi_{\text{inc}}^{(1)}(\boldsymbol{r})\big]dx \tag{3}$$

where $\mathcal{R}_\pm(\chi_1) = 1 \pm \mathcal{R}(\chi_1)$.

Due to the refraction phenomenon, the scattered field $\psi_{\text{sca}}^{(1)}$ induces new surface currents of the second order, which form the second bound on the surface. The newly generated currents can be again expressed from PO [here the scattered field becomes the incident field for the second-order surface currents, $\forall \boldsymbol{r} \in \Sigma$, $\psi_{\text{sca}}^{(1)}(\boldsymbol{r}) = \psi_{\text{inc}}^{(2)}(\boldsymbol{r})$]. Therefore, we can write

$$\begin{cases} \psi^{(2)}(\boldsymbol{r}) = [1 + \mathcal{R}(\chi_2)]\psi_{\text{sca}}^{(1)}(\boldsymbol{r}) \\ \partial_n \psi^{(2)}(\boldsymbol{r}) = [1 - \mathcal{R}(\chi_2)]\partial_n \psi_{\text{sca}}^{(1)}(\boldsymbol{r}). \end{cases} \tag{4}$$

Then, these currents can be used to calculate the second-order scattered field. Analogously, this process is again iterated at higher orders. Hence, the scattered field of the order m $(m \geq 1)$ can be written as follows:

$$\psi_{\text{sca}}^{(m)}(\boldsymbol{r}') = \int_x \big[\mathcal{R}_+(\chi_m)\psi_{\text{inc}}^{(m)}(\boldsymbol{r})\partial_n g(\boldsymbol{r}, \boldsymbol{r}') - \mathcal{R}_-(\chi_m)g(\boldsymbol{r}, \boldsymbol{r}')\partial_n \psi_{\text{inc}}^{(m)}(\boldsymbol{r})\big]dx \tag{5}$$

where the surface currents $\{\psi^{(m)}(\boldsymbol{r}), \partial_n \psi^{(m)}(\boldsymbol{r})\}$ satisfy the generalized PO approximation

$$\begin{cases} \psi^{(m)}(\boldsymbol{r}) = [1 + \mathcal{R}(\chi_m)]\psi_{\text{sca}}^{(\text{m-1})}(\boldsymbol{r}) \\ \partial_n \psi^{(m)}(\boldsymbol{r}) = [1 - \mathcal{R}(\chi_m)]\partial_n \psi_{\text{sca}}^{(\text{m-1})}(\boldsymbol{r}) \end{cases} \tag{6}$$

where χ_m is the local incidence angle at the mth rebound.

Finally, the field scattered by the rough surface inside $\mathbf{\Omega}_2$ up to the order M can be obtained by

$$\psi_{\text{sca}}(\boldsymbol{r}') = \sum_{i=1}^{M} \psi_{\text{sca}}^{(i)}(\boldsymbol{r}'). \tag{7}$$

B. Incident Field

The incident field ψ_{inc} on the rough surface $r \in \Sigma$ can be defined as [11]

$$\psi_{\text{inc}}(\boldsymbol{r}) \approx -2jk_0 \int_{S_a} \psi_{\text{inc}}^a(\boldsymbol{r}_a)g(\boldsymbol{r}_a, \boldsymbol{r})dS_a \tag{8}$$

where $\psi_{\text{inc}}^a(\boldsymbol{r}_a)$ is the initial field on a vertical surface (transmitting antenna) $S_a = \{z_a \in [z_{a,\min}; z_{a,\max}], x_a = 0\}$ with x_a being the constant abscissa and z_a its heights. Therefore, the incident field ψ_{inc} is defined as the field produced by the source that would exist in the duct in the absence of the rough surface. The incident field on the rough surface is then evaluated by propagating the initial field from the vertical plane onto the rough surface using the ducting medium propagator. A possible candidate for the expression of ψ_{inc}^a is [13]

$$\psi_{\text{inc}}^a(z_a) = \frac{1}{\sqrt{\pi}\,\Delta\theta} \int_{-\pi/2}^{+\pi/2} e^{-\frac{(\theta-\theta_{\text{inc}})^2}{(\Delta\theta)^2}} e^{jk_0(z_a - z_{a,0})\cos\theta} d\theta \tag{9}$$

where $\psi_{\text{inc}}^{a}(z_a)$ is the incident field on the vertical surface S_a, i.e., the transmitting antenna (z_a varies); $z_{a,0}$ is the center of the antenna, a constant number with respect to z (the abscissa of the antenna x_a is set to zero); θ_{inc} is the incidence angle measured from the positive z-axis; and $\Delta\theta = 2/(k_0 G) = 2/(k_0 g_z \sin\theta_{\text{inc}})$, in which G is the transverse width of the beam (perpendicular to the propagation axis) and g_z is the vertical footprint (in the $x = 0$ vertical plane).

If the integration in (9) is performed in an exact manner, ψ_{inc}^{a} satisfies the Helmholtz wave equation exactly. The field is then qualified as Maxwellian. In [11], a closed-form expression of (9) is given to avoid the numerical integration over θ.

III. Coherent Surface Currents

Since the sea surface height is a random variable, the surface currents expressed from (1) are also random variables. Hence, it is possible to calculate their statistical moments such as the coherent (first-order statistical moment) and incoherent (second-order statistical moment) components of the surface currents.

Under the PWE approximation and for a medium of square refractive index equal to $n^2(z) = 1 + \varepsilon(h - z), \zeta(x) < z < h$, the spatial Green function g can be written as [11], [14]

$$g(\boldsymbol{r}, \boldsymbol{r}') = f(X)s(X, z, z') \tag{10}$$

where

$$\begin{cases} f(X) = \dfrac{e^{j\pi/4}}{2\sqrt{2\pi k_0 X}} e^{jk_0\left(X + \frac{\varepsilon X h}{2} - \frac{\varepsilon^2 X^3}{96}\right)} \\ s(X, z, z') = e^{jk_0\left[\frac{(z-z')^2}{2X} - \frac{\varepsilon X(z+z')}{4}\right]} \end{cases} \tag{11}$$

with k_0 the incident wavenumber and $X = |x - x'|$ the horizontal distance between the source point and the observation point.

In all the calculations to follow, we assume the sea surface to be a perfect electric conductor and consider both TM and TE polarizations.

A. TM Polarization

By convention, the Fresnel reflection coefficient for a PC surface and TM polarization is $\mathcal{R} = 1$. The coherent surface current of the order m ($m \geq 1$) is defined as

$$\Psi_{\text{coh}}^{(m)} = \langle \psi^{(m)}(\boldsymbol{r}_m) \rangle \tag{12}$$

where the symbol $\langle \bullet \rangle$ is the ensemble average operator that operates on the random variables of $\psi^{(m)}(\boldsymbol{r}_m)$.

1) First Order: For the first order, the substitution of (10) and (8) into (1) leads to

$$\begin{aligned} \Psi_{\text{coh}}^{(1)} &= \langle \psi^{(1)}(\boldsymbol{r}_1) \rangle \\ &= \left\langle -4jk_0 \int \psi_{\text{inc}}^{a}(\boldsymbol{r}_a) g(\boldsymbol{r}_a, \boldsymbol{r}_1) dS_a \right\rangle \\ &= -4jk_0 \int \psi_{\text{inc}}^{a}(\boldsymbol{r}_a) \langle f(X_1) s(X_1, z_a, \zeta_1) \rangle dS_a \end{aligned} \tag{13}$$

where $X_1 = |x_a - x_1|$ is the horizontal distance between the transmitting antenna and the first rebound. $s_1 = s(X_1, z_a, \zeta_1)$ is a random variable (which depends on the height of the surface ζ_1), and $f_1 = f(X_1)$ is a deterministic function. Therefore, (13) requires only the calculation of the ensemble average of s_1, which can be written as $s(\zeta_1) = \exp(-a\zeta_1^2 + 2b\zeta_1 + c)$, in which

$$\begin{cases} a = -\dfrac{jk_0}{2X_1} \\ b = -\dfrac{jk_0}{2}\left(\dfrac{z_a}{X_1} + \dfrac{\varepsilon X_1}{4}\right) \\ c = \dfrac{jk_0}{2}\left(\dfrac{z_a^2}{X_1} - \dfrac{\varepsilon X_1 z_a}{2}\right). \end{cases} \tag{14}$$

Assuming that the random variable ζ_1 is normally distributed with zero mean and surface height variance σ_ζ^2, the ensemble average is obtained by the following expression:

$$\langle s(\zeta_1) \rangle = u_\zeta e^{c - \frac{1}{2}u_\zeta^2 k_0^2 \sigma_\zeta^2 \cot^2\theta_1} \tag{15}$$

where

$$u_\zeta = \frac{1}{\sqrt{1 - jk_0\sigma_\zeta^2/X_1}} \tag{16}$$

and

$$\cot\theta_1 = \frac{z_a}{X_1} + \frac{\varepsilon X_1}{4}. \tag{17}$$

The incidence angle on the surface of the first bound θ_1 is defined with respect to the z-direction.

Finally, for the first-order coherent surface current, we obtain

$$\begin{aligned} \Psi_{\text{coh}}^{(1)} \approx -4jk_0 \int_{S_a} \psi_{\text{inc}}^{a}(\boldsymbol{r}_a) f_1 e^{\frac{jk_0}{2}\left(\frac{z_a^2}{X_1} - \frac{\varepsilon X_1 z_a}{2}\right)} \\ \times u_\zeta e^{-\frac{1}{2}u_\zeta^2 k_0^2 \sigma_\zeta^2 \cot^2\theta_1} dS_a. \end{aligned} \tag{18}$$

In the flat surface case ($\zeta_1, \gamma_1 = 0, \forall \boldsymbol{r}_1 \in \Sigma$), for the first-order surface current, we have

$$\Psi_{\text{flat}}^{(1)} \approx -4jk_0 \int_{S_a} \psi_{\text{inc}}^{a}(\boldsymbol{r}_a) f_1 e^{\frac{jk_0}{2}\left(\frac{z_a^2}{X_1} - \frac{\varepsilon X_1 z_a}{2}\right)} dS_a. \tag{19}$$

For practical applications, the order of magnitude of the duct parameter is $\varepsilon \approx 10^{-5}$ and the variations of the local incidence angle $\theta_1 \to \pi/2$ with respect to the horizontal distance of the first rebound from the surface (when $X_1 \gg z_a$) are negligible, i.e., the incidence angle can be considered as constant. Furthermore, the standard deviation σ_ζ of the surface heights of the wind-roughened sea surfaces for a wind speed up to $u_{10} = 5$ m/s does not exceed 0.16 m [15]. Hence, the coefficient u_ζ can be considered as constant and equal to 1 for radar microwave frequencies. Therefore, from (11) and (18), the first-order coherent current on the surface becomes

$$\Psi_{\text{coh}}^{(1)} \approx e^{-R_{a,1}^2} \times \Psi_{\text{flat}}^{(1)} \tag{20}$$

where

$$R_{a,1} = \frac{k_0 \sigma_\zeta \cot\theta_1}{\sqrt{2}}. \tag{21}$$

In (20), the first term corresponds to an attenuation coefficient due to the surface roughness, and the second term is the current on a flat surface expressed by (19). From a ray approach of the geometrical optics [16], [17] and for a linear-square refractive index profile, the equation of the ray trajectory is a parabola, and it is easy to show that the incidence angle of the first bound is θ_1 defined by (17). Since for low-grazing angles ($|\theta_1| \to \pi/2$), $\cot\theta_1 \approx \cos\theta_1$, the parameter $R_{a,1}$ of the attenuation coefficient reduces to the Rayleigh parameter of the well-known Ament model, defined in [1], divided by $\sqrt{2}$. Indeed, Ament considered the coherent scattered field instead of the coherent surface current [see (47) and (48)].

2) Second Order: From (4), the second-order coherent surface current is

$$\Psi_{\text{coh}}^{(2)} = \langle \psi^{(2)}(\boldsymbol{r}_2)\rangle = 2\left\langle \int \psi^{(1)}(\boldsymbol{r}_2)\partial_{n_1} g(\boldsymbol{r}_1, \boldsymbol{r}_2)dx_1 \right\rangle \tag{22}$$

and eventually

$$\Psi_{\text{coh}}^{(2)} \approx -8jk_0 \iint \langle \psi_{\text{inc}}^a(\boldsymbol{r}_a) g(\boldsymbol{r}_a, \boldsymbol{r}_1) \times \partial_{n_1} g(\boldsymbol{r}_1, \boldsymbol{r}_2)dx_1 dS_a\rangle. \tag{23}$$

The detailed calculation of the second-order coherent current on the surface is reported in Appendix A. The final result is obtained under the following assumptions.

1) The random variables ζ_i and γ_i, at the same point $\boldsymbol{r}_i$, $i \in [1, 2]$, are statistically independent.
2) The random variables (ζ_1, γ_1) and (ζ_2, γ_2) at two distinct points on the surface (e.g., points of the successive rebounds $\boldsymbol{r}_1$ and $\boldsymbol{r}_2$) are uncorrelated.
3) The surface height standard deviation meets the following conditions: $\sigma_\zeta \ll (X_1/k_0)^{1/2}$ and $\sigma_\zeta \ll (X_2/k_0)^{1/2}$, where $X_2 = |x_1 - x_2|$ is the horizontal distance between the points of the first and second rebounds and $X_1 = |x_a - x_1|$ the horizontal distance between the point of the first rebound and the source.

Thus, the second-order coherent surface current is given by

$$\Psi_{\text{coh}}^{(2)} \approx -8k_0^2 \int_{S_a}\int_{x_1} \psi_{\text{inc}}^a(\boldsymbol{r}_a) f_1 f_2 \cot\theta_2 e^{\frac{jk_0}{2}\left(\frac{z_a^2}{X_1} - \frac{\varepsilon X_1 z_a}{2}\right)} \times e^{-(R_{a,1}+R_{a,2})^2 - R_{a,2}^2} e^{\frac{jk_0^2\sigma_\zeta^3\varepsilon}{2\sqrt{2}}(R_{a,1}+R_{a,2})} dx_1 dS_a \tag{24}$$

where $R_{a,1}$ and $R_{a,2}$ correspond to the Rayleigh roughness parameter divided by $\sqrt{2}$, defined by (21), and

$$R_{a,2} = \frac{k_0\sigma_\zeta \cot\theta_2}{\sqrt{2}} \tag{25}$$

respectively, with the incidence angle θ_2 calculated by the ray approach

$$\cot\theta_2 = \frac{\varepsilon X_2}{4}. \tag{26}$$

Again, it is possible to find a relationship between the second-order current on the flat surface and the coherent current on the random rough surface under certain conditions. Considering that the local incidence angles of the first and second rebounds can be assumed to be constant (independent of the integration variables), we can write

$$\Psi_{\text{coh}}^{(2)} \approx e^{-(R_{a,1}+R_{a,2})^2 - R_{a,2}^2} e^{\frac{jk_0^2\sigma_\zeta^3\varepsilon}{2\sqrt{2}}(R_{a,1}+R_{a,2})} \times \Psi_{\text{flat}}^{(2)} \tag{27}$$

where $\Psi_{\text{flat}}^{(2)}$ is the second-order current on the flat surface given by

$$\Psi_{\text{flat}}^{(2)} \approx -8k_0^2 \iint \psi_{\text{inc}}^a(\boldsymbol{r}_a) f_1 f_2 \cot\theta_2 e^{\frac{jk_0}{2}\left(\frac{z_a^2}{X_1} - \frac{\varepsilon X_1 z_a}{2}\right)} dx_1 dS_a. \tag{28}$$

The obtained coefficient in (27), which multiplies the flat surface current, characterizes the surface roughness impact on the current after two reflections from the sea surface in the given stratified medium. We observe a term that corresponds to the attenuation predicted by applying the Ament model for each rebound. Moreover, there is a term that shows a slight correction in phase. It is dependent on the duct parameter, which means that it is linked to the refraction phenomenon and to the surface roughness. It comes from a sort of a correlation between the different points of the first and second rebounds.

If in (22), the random variable $g(\boldsymbol{r}_a, \boldsymbol{r}_1)$ is substituted for its ensemble average (20) and then $g(\boldsymbol{r}_1, \boldsymbol{r}_2)$ substituted for $g(\boldsymbol{r}_1, \boldsymbol{r}_2)|_{\zeta_1=0}$, then in (27), the exponential term, accounting for the surface roughness, becomes $e^{-(R_{a,1}+R_{a,2})^2}$, which is very different (in particular, there is no phase term). This means that the statistical correlation between the first-order surface current and $g(\boldsymbol{r}_1, \boldsymbol{r}_2)$ must be accounted for the calculation of the ensemble average.

Usually, when the PWE approach is used to compute the scattered field, the boundary condition is introduced via a reflection coefficient, which is often the Ament coefficient (when the surface roughness is considered). This means that for the introduction of the boundary condition in the PWE, the ensemble average is already made. Then, it was implicitly assumed that the current on the surface and the propagation phenomenon are statistically uncorrelated. From (27), this assumption is satisfied if the phase factor is close to unity.

3) mth Order: From (4), by assuming that $\zeta_1, \zeta_2, \ldots, \zeta_m$ are uncorrelated, the coherent surface current of the mth ($m \geq 2$) order is

$$\Psi_{\text{coh}}^{(m)} = \langle \psi^{(m)}(\boldsymbol{r}_m)\rangle = (-2jk_0)2^m \int \cdots \int \psi_{\text{inc}}^a(\boldsymbol{r}_a) \times \langle g(\boldsymbol{r}_a, \boldsymbol{r}_1)\partial_n g(\boldsymbol{r}_1, \boldsymbol{r}_2)\ldots\partial_n g(\boldsymbol{r}_{m-1}, \boldsymbol{r}_m)\rangle \times dx_{m-1}\ldots dx_1 dS_a. \tag{29}$$

The calculation of the ensemble average is similar to the previous one and is given in Appendix B. Hence, the following assumptions are made.

1) The random variables ζ_i and γ_i, at the same point $\boldsymbol{r}_i$, $i \in [1, m]$, are statistically independent.
2) The random variables (ζ_i, γ_i) and (ζ_j, γ_j) at two distinct points on the surface (e.g., points of two distinct rebounds $\boldsymbol{r}_i$ and $\boldsymbol{r}_j$, $i \neq j$) are uncorrelated.
3) The surface height standard deviation meets the condition $\sigma_\zeta \ll (X_i/k_0)^{1/2}, i \in [1, m]$, where

$X_i = |x_{i-1} - x_i|$ is the horizontal distance between two successive rebounds.

Under the above-mentioned assumptions, we show that the coherent surface current of the mth order is

$$\Psi_{\text{coh}}^{(m)} \approx 2(-2jk_0)^m \int \cdots \int \psi_{\text{inc}}^a(\boldsymbol{r}_a) f_1 \prod_{k=2}^{m} f_k \cot\theta_k \times e^{\frac{jk_0}{2}\left(\frac{z_a^2}{X_1} - \frac{\varepsilon X_1 z_a}{2}\right)} e^{-R_{a,m}^2 - \sum_{i=1}^{m-1}(R_{a,i}+R_{a,i+1})^2} \times e^{\frac{jk_0^2\sigma_\zeta^3\varepsilon}{2\sqrt{2}} \sum_{j=2}^{m-1} R_{a,j}\left(1+\frac{R_{a,j-1}}{R_{a,j}}\right)\left(1+\frac{R_{a,j+1}}{R_{a,j}}\right)} \times e^{\frac{jk_0^2\sigma_\zeta^3\varepsilon}{2\sqrt{2}}(R_{a,m-1}+R_{a,m})} dx_{m-1}\ldots dx_1 dS_a \tag{30}$$

where $\Psi_{\text{flat}}^{(m)}$ is the coherent current on a flat surface of the order m expressed as

$$\Psi_{\text{flat}}^{(m)} \approx 2\,(-2jk_0)^m \int \cdots \int \psi_{\text{inc}}^a(\boldsymbol{r}_a) f_1 \prod_{k=2}^{m} f_k \cot\theta_k \times e^{\frac{jk_0}{2}\left(\frac{z_a^2}{X_1} - \frac{\varepsilon X_1 z_a}{2}\right)} dx_{m-1}\ldots dx_1 dS_a \tag{31}$$

and

$$\begin{cases} \cot\theta_k = \dfrac{\varepsilon X_{k-1}}{4}, & \text{with } k \geq 2 \\ R_{a,k} = \dfrac{k_0\sigma_\zeta \cot\theta_k}{\sqrt{2}}. \end{cases} \tag{32}$$

Once more, if we assume that the local incidence angles of all rebounds are constant, we can derive a relationship between the coherent surface current and the current on the flat surface as follows:

$$\Psi_{\text{coh}}^{(m)} \approx e^{-R_{a,m}^2 - \sum_{i=1}^{m-1}(R_{a,i}+R_{a,i+1})^2} \times e^{\frac{jk_0^2\sigma_\zeta^3\varepsilon}{2\sqrt{2}} \sum_{j=2}^{m-1} R_{a,j}\left(1+\frac{R_{a,j-1}}{R_{a,j}}\right)\left(1+\frac{R_{a,j+1}}{R_{a,j}}\right)} \times e^{\frac{jk_0^2\sigma_\zeta^3\varepsilon}{2\sqrt{2}}(R_{a,m-1}+R_{a,m})} \times \Psi_{\text{flat}}^{(m)}. \tag{33}$$

The last equation gives the generalized roughness parameter for m ($m \geq 2$) rebounds from the sea surface in a stratified medium concerning the surface currents. The first line of (33) is an attenuation factor, meaning that the modulus of the coherent surface current is smaller than that obtained for a flat surface. In addition, as the number of bounces increases, as expected the attenuation factor decreases. This factor corresponds to the Rayleigh roughness parameter that was predicted by the Ament model [1] for one rebound and within free space. The last two lines of (33) show that the phase is also modified by the surface roughness at each surface reflection starting from the second one and that it depends on the duct parameter ε.

B. TE Polarization

In the same way, we can derive the expressions for the coherent surface currents and scattered field for vertically polarized waves. Assuming a PC sea surface, the Fresnel reflection coefficient is, by convention, $\mathcal{R} = -1$.

Therefore, the coherent surface current of the order m ($m \geq 1$) is defined by

$$\Psi_{\text{coh}}^{(m)} = \langle \partial_n \psi^{(m)}(\boldsymbol{r}_m)\rangle \tag{34}$$

which, again, describes the ensemble average operation over the random variables of $\partial_n \psi^{(m)}(\boldsymbol{r}_m)$.

1) First Order: By substituting (8) and (10) into (1), the first-order coherent surface current becomes

$$\begin{aligned}\Psi_{\text{coh}}^{(1)} &= \langle \partial_{n_1}\psi^{(1)}(\boldsymbol{r}_1)\rangle \\ &= \left\langle -4jk_0 \int \psi_{\text{inc}}^a(\boldsymbol{r}_a)\partial_{n_1} g(\boldsymbol{r}_a, \boldsymbol{r}_1) dS_a \right\rangle \\ &= -4jk_0 \int \psi_{\text{inc}}^a(\boldsymbol{r}_a)\langle f(X_1)\partial_{n_1} s(X_1, z_a, \zeta_1)\rangle dS_a. \end{aligned} \tag{35}$$

After solving this integration and assuming that the random variables ζ_1 and γ_1 are statistically independent, analogously to the TM case, the first-order coherent surface current is obtained by

$$\Psi_{\text{coh}}^{(1)} \approx -4k_0^2 \int_{S_a} \psi_{\text{inc}}^a(\boldsymbol{r}_a) f_1 \cot\theta_1 e^{\frac{jk_2}{2}\left(\frac{z_a^2}{X_1} - \frac{\varepsilon X_1 z_a}{2}\right)} \times e^{-R_{a,1}^2} dS_a. \tag{36}$$

Finally, if we assume that the local incidence angle θ_1 is constant, with respect to the horizontal distance, far from the transmitter, we obtain the same relationship between the coherent current on the rough surface and the current on the flat surface of the first order like in the TM case, given by (20). The appropriate flat surface current is expressed by the following equation:

$$\Psi_{\text{flat}}^{(1)} \approx -4k_0^2 \int_{S_a} \psi_{\text{inc}}^a(\boldsymbol{r}_a) f_1 \cot\theta_1 e^{\frac{jk_0}{2}\left(\frac{z_a^2}{X_1} - \frac{\varepsilon X_1 z_a}{2}\right)} dS_a. \tag{37}$$

2) Second Order: From (4), the second-order coherent surface current is then

$$\begin{aligned}\Psi_{\text{coh}}^{(2)} &= \langle \partial_{n_2}\psi^{(2)}(\boldsymbol{r}_2)\rangle \\ &= -2\left\langle \partial_{n_2} \int \partial_{n_1}\psi^{(1)}(\boldsymbol{r}_2) g(\boldsymbol{r}_1, \boldsymbol{r}_2) dx_1 \right\rangle \\ &= 8jk_0 \iint \psi_{\text{inc}}^a(\boldsymbol{r}_a)\langle \partial_{n_1} g(\boldsymbol{r}_a, \boldsymbol{r}_1) \\ &\quad \times \partial_{n_2} g(\boldsymbol{r}_1, \boldsymbol{r}_2)\rangle dx_1 dS_a. \end{aligned} \tag{38}$$

By introducing the same assumptions on the random variables ζ_i and γ_i, $i \in [1, 2]$, like in the TM case, and after applying the same way as that in Appendix A, we obtain the expression for the second-order coherent surface current. Then, considering that the local incidence angles are constant, we obtain the same relationship as in the TM case, given by (27), the only difference being the expression for the current on the flat surface given by

$$\Psi_{\text{flat}}^{(2)} \approx -8jk_0^3 \int_{S_a}\int_{x_1} \psi_{\text{inc}}^a(\boldsymbol{r}_a) f_1 f_2 \cot\theta_1 \cot\theta_2 \times e^{\frac{jk_0}{2}\left(\frac{z_a^2}{X_1} - \frac{\varepsilon X_1 z_a}{2}\right)} dS_a dx_1. \tag{39}$$

3) mth Order: Using the same way and with the same assumptions as for TM polarization, we obtain the coherent surface current of the mth order ($m \geq 2$) and derive it as a function of the current on the flat surface like in (33). In this case, the current on the flat surface is given by

$$\Psi_{\text{flat}}^{(m)} \approx (2jk_0)^{m+1} \int \cdots \int \psi_{\text{inc}}^{a}(\boldsymbol{r}_a) \prod_{k=1}^{m} f_k \cot\theta_k \times e^{\frac{jk_0}{2}\left(\frac{z_a^2}{X_1} - \frac{\varepsilon X_1 z_a}{2}\right)} dx_{m-1} \ldots dx_1 dS_a. \tag{40}$$

IV. Coherent Scattered Field

Using the same way, we can derive the expressions for the field scattered from the surface. The coherent scattered field of the order m ($m \geq 1$) is defined as

$$\Psi_{\text{sca,coh}}^{(m)} = \left\langle \psi_{\text{sca}}^{(m)}(\boldsymbol{r}'_m) \right\rangle \tag{41}$$

where $\psi_{\text{sca}}^{m}(\boldsymbol{r}'_m)$ is the scattered field of the order m and at the point $\boldsymbol{r}'_m \in \boldsymbol{\Omega}_2$, given by (5).

A. TM Polarization

1) First Order: Analogously to the coherent surface current, the first-order coherent scattered field is defined as

$$\Psi_{\text{coh,sca}}^{(1)} = \left\langle \psi_{\text{sca}}^{(1)}(\boldsymbol{r}'_1) \right\rangle = -4jk_0 \iint \psi_{\text{inc}}^{a}(\boldsymbol{r}_a) \times \langle g(\boldsymbol{r}_a, \boldsymbol{r}_1) \partial_{n_1} g(\boldsymbol{r}_1, \boldsymbol{r}'_1) \rangle dx_1 dS_a. \tag{42}$$

The calculation of the coherent scattered field is similar to the calculation of the coherent surface currents. Hence, we present the final expression with the following assumptions.

1) The random variables ζ_1 and γ_1, at the point $\boldsymbol{r}_1$, are statistically independent.
2) The surface height standard deviation σ_ζ satisfies the following conditions: $\sigma_\zeta \ll (X_1/k_0)^{1/2}$ and $\sigma_\zeta \ll (X'_1/k_0)^{1/2}$, where $X'_1 = |x_1 - x'_1|$ is the horizontal distance between the point of the first rebound and the observation point.

Thus, the first-order coherent scattered field is obtained by

$$\Psi_{\text{sca,coh}}^{(1)} \approx -4k_0^2 \int_{S_a} \int_{x_1} \psi_{\text{inc}}^{a}(\boldsymbol{r}_a) f_1 f'_1 \cot\theta'_1 \times e^{\frac{jk_0}{2}\left(\frac{z_a^2}{X_1} - \frac{\varepsilon X_1 z_a}{2}\right)} e^{\frac{jk_0}{2}\left(\frac{z_1'^2}{X'_1} - \frac{\varepsilon X'_1 z'_1}{2}\right)} \times e^{-(R_{a,1}+R'_{a,1})^2} dx_1 dS_a \tag{43}$$

where

$$\begin{cases} R_{a,1} = \dfrac{k_0\sigma_\zeta \cot\theta_1}{\sqrt{2}} = \dfrac{k_0\sigma_\zeta}{\sqrt{2}}\left(\dfrac{z_a}{X_a} + \dfrac{\varepsilon X_a}{4}\right) \\ R'_{a,1} = \dfrac{k_0\sigma_\zeta \cot\theta'_1}{\sqrt{2}} = \dfrac{k_0\sigma_\zeta}{\sqrt{2}}\left(\dfrac{z'_1}{X'_1} + \dfrac{\varepsilon X'_1}{4}\right) \end{cases} \tag{44}$$

and $X_1 = |x_a - x_1|$ and $X'_1 = |x_1 - x'_1|$.

Assuming that the incidence and reflection angles are constant, we can derive a relationship between the coherent scattered field and the field reflected by the corresponding flat surface as follows:

$$\Psi_{\text{sca,coh}}^{(1)} \approx e^{-(R_{a,1}+R'_{a,1})^2} \Psi_{\text{sca,flat}}^{(1)} \tag{45}$$

where

$$\Psi_{\text{sca,flat}}^{(1)} \approx -4k_0^2 \int_{S_a} \int_{x_1} \psi_{\text{inc}}^{a}(\boldsymbol{r}_a) f_1 f'_1 \cot\theta'_1 \times e^{\frac{jk_0}{2}\left(\frac{z_a^2}{X_1} - \frac{\varepsilon X_1 z_a}{2}\right)} e^{\frac{jk_0}{2}\left(\frac{z_1'^2}{X'_1} - \frac{\varepsilon X'_1 z'_1}{2}\right)} dx_1 dS_a. \tag{46}$$

Now, assuming that the incidence and reflection angle, θ_1 and θ'_1, on the surface are equal, we obtain the following relationship:

$$\Psi_{\text{sca,coh}}^{(1)} \approx e^{-4R_{a,1}^2} \Psi_{\text{sca,flat}}^{(1)}. \tag{47}$$

By introducing the Rayleigh roughness parameter of the Ament model defined as $R_a = k_0\sigma_\zeta \cot\theta_1 = \sqrt{2}R_{a,1}$, we obtain

$$\Psi_{\text{sca,coh}}^{(1)} \approx^{-2R_a^2} \Psi_{\text{sca,flat}}^{(1)}. \tag{48}$$

Thus, it is demonstrated that the Ament model is a particular case of the PO approximation. As shown in the following, the PO allows us to generalize the derivation of this coefficient to multiple rebounds and for a stratified medium. Within the Rayleigh parameter, $\cos\theta_1$ is replaced by $\cot\theta_1$ (calculated from the geometrical optics), knowing that, for low-grazing angles, we have $\cot\theta \approx \cos\theta$.

2) Second Order: Using the same way as in the previous section, we can show that the second-order coherent scattered field is

$$\Psi_{\text{sca,coh}}^{(2)} \approx 8jk_0^3 \iiint \psi_{\text{inc}}^{a}(\boldsymbol{r}_a) f_1 f_2 f'_2 \cot\theta_2 \cot\theta'_2 \times e^{\frac{jk_0}{2}\left(\frac{z_a^2}{X_1} - \frac{\varepsilon X_1 z_a}{2}\right)} e^{\frac{jk_0}{2}\left(\frac{z_2'^2}{X'_2} - \frac{\varepsilon X'_2 z'_2}{2}\right)} \times e^{-(R_{a,1}+R_{a,2})^2 - (R_{a,2}+R'_{a,2})^2} \times e^{\frac{jk_0^2\sigma_\zeta^3\varepsilon}{2\sqrt{2}} R_{a,2}\left(1+\frac{R_{a,1}}{R_{a,2}}\right)\left(1+\frac{R'_{a,2}}{R_{a,2}}\right)} dx_2 dx_1 dS_a \tag{49}$$

where the coefficients $R_{a,2}$ and $R'_{a,2}$ are given by

$$\begin{cases} R_{a,2} = \dfrac{k_0\sigma_\zeta \cot\theta_2}{\sqrt{2}} = \dfrac{k_0\sigma_\zeta}{\sqrt{2}} \dfrac{\varepsilon X_2}{4} \\ R'_{a,2} = \dfrac{k_0\sigma_\zeta \cot\theta'_2}{\sqrt{2}} = \dfrac{k_0\sigma_\zeta}{\sqrt{2}}\left(\dfrac{z'_2}{X'_2} + \dfrac{\varepsilon X'_2}{4}\right). \end{cases} \tag{50}$$

Once again, assuming that the incidence and reflection angles of both reflections are independent of the variables of integration, we can derive the following relationship between the coherent scattered field and the field reflected by the corresponding flat surface:

$$\Psi_{\text{sca,coh}}^{(2)} \approx e^{-(R_{a,1}+R_{a,2})^2 - (R_{a,2}+R'_{a,2})^2} \times e^{\frac{jk_0^2\sigma_\zeta^3\varepsilon}{2\sqrt{2}} R_{a,2}\left(1+\frac{R_{a,1}}{R_{a,2}}\right)\left(1+\frac{R'_{a,2}}{R_{a,2}}\right)} \times \Psi_{\text{sca,flat}}^{(2)} \tag{51}$$

where

$$\Psi_{\text{sca,flat}}^{(2)} \approx 8jk_0^3 \iiint \psi_{\text{inc}}^{a}(\boldsymbol{r}_a) f_1 f_2 f'_2 \cot\theta_2 \cot\theta'_2 \times e^{\frac{jk_0}{2}\left(\frac{z_a^2}{X_1} - \frac{\varepsilon X_1 z_a}{2}\right)} e^{\frac{jk_0}{2}\left(\frac{z_2'^2}{X'_2} - \frac{\varepsilon X'_2 z'_2}{2}\right)} dx_2 dx_1 dS_a. \tag{52}$$

Assuming that the incidence and reflection angles of both reflections are equal ($\theta_1 = \theta_2$), we obtain

$$\Psi^{(2)}_{\text{sca,coh}} \approx e^{-4R_a^2} e^{jk_0^2\sigma_\zeta^3\varepsilon R_a}\Psi^{(2)}_{\text{sca,flat}}. \tag{53}$$

We can observe a term that corresponds to the Ament model for two successive reflections and, again, a phase correction term like in the case of the coherent surface currents. The last equation represents the Ament model extended to an inhomogeneous medium of linear-square refraction index profile.

3) mth Order: Using the same way as in the previous section, we can show that the coherent scattered field of the order m ($m \geq 2$) is

$$\begin{aligned}\Psi^{(m)}_{\text{sca,coh}} \approx (-2jk_0)^{m+1} &\int \cdots \int \psi^a_{\text{inc}}(\boldsymbol{r}_a) f_1 \prod_{k=2}^{m} f_k \cot\theta_k \\ &\times f'_m \cot\theta'_m e^{\frac{jk_0}{2}\left(\frac{z_a^2}{X_1}-\frac{\varepsilon X_1 z_a}{2}\right)} e^{\frac{jk_0}{2}\left(\frac{z_m'^2}{X'_m}-\frac{\varepsilon X'_m z'_m}{2}\right)} \\ &\times e^{-\sum_{i=1}^{m-1}(R_{a,i}+R_{a,i+1})^2-(R_{a,m}+R'_{a,m})^2} \\ &\times e^{\frac{jk_0^2\sigma_\zeta^3\varepsilon}{2\sqrt{2}}\sum_{j=2}^{m-1} R_{a,j}\left(1+\frac{R_{a,j-1}}{R_{a,j}}\right)\left(1+\frac{R_{a,j+1}}{R_{a,j}}\right)} \\ &\times e^{\frac{jk_0^2\sigma_\zeta^3\varepsilon}{2\sqrt{2}} R_{a,m}\left(1+\frac{R_{a,m-1}}{R_{a,m}}\right)\left(1+\frac{R'_{a,m}}{R_{a,m}}\right)} dx_m \cdots dS_a.\end{aligned} \tag{54}$$

Considering the local incidence and reflection angles independent of the integration variables, we can establish a relationship between the coherent scattered field and the field reflected by the corresponding flat surface of the mth order as follows:

$$\begin{aligned}\Psi^{(m)}_{\text{sca,coh}} \approx\; & e^{-\sum_{i=1}^{m-1}(R_{a,i}+R_{a,i+1})^2-(R_{a,m}+R'_{a,m})^2} \\ &\times e^{\frac{jk_0^2\sigma_\zeta^3\varepsilon}{2\sqrt{2}}\sum_{j=2}^{m-1} R_{a,j}\left(1+\frac{R_{a,j-1}}{R_{a,j}}\right)\left(1+\frac{R_{a,j+1}}{R_{a,j}}\right)} \\ &\times e^{\frac{jk_0^2\sigma_\zeta^3\varepsilon}{2\sqrt{2}} R_{a,m}\left(1+\frac{R_{a,m-1}}{R_{a,m}}\right)\left(1+\frac{R'_{a,m}}{R_{a,m}}\right)} \times \Psi^{(m)}_{\text{sca,flat}}\end{aligned} \tag{55}$$

with

$$\begin{aligned}\Psi^{(m)}_{\text{sca,flat}} \approx (-2jk_0)^{m+1} &\int \cdots \int \psi^a_{\text{inc}}(\boldsymbol{r}_a) \\ &\times f_1 \prod_{k=2}^{m} f_k \cot\theta_k f'_m \cot\theta'_m e^{\frac{jk_0}{2}\left(\frac{z_a^2}{X_1}-\frac{\varepsilon X_1 z_a}{2}\right)} \\ &\times e^{\frac{jk_0}{2}\left(\frac{z_m'^2}{X'_m}-\frac{\varepsilon X'_m z'_m}{2}\right)} dx_m \cdots dS_a.\end{aligned} \tag{56}$$

Equation (55) represents the generalized roughness parameter for multiple reflections from the rough sea surface in a stratified medium. The first line corresponds to the multiple application of the Ament surface roughness model for multiple reflections (assuming that the local incidence and reflection angles are equal). However, the PO method shows that there is a phase correction term for multiple reflected fields from the random rough surface, which depends on the duct parameter ε.

B. TE Polarization

The same calculations can be done for the coherent scattered field for TE polarization. The relationship between the coherent scattered field above the rough surface and the field reflected above the corresponding flat surface, which was previously derived for TM polarized waves, is still valid. Therefore, we give only the equations of the reflected field above the flat surface.

1) First Order:

$$\begin{aligned}\Psi^{(1)}_{\text{sca,flat}} \approx 4k_0^2 &\int_{S_a}\int_{x_1} \psi^a_{\text{inc}}(\boldsymbol{r}_a) f_1 f'_1 \cot\theta_1 \\ &\times e^{\frac{jk_0}{2}\left(\frac{z_a^2}{X_1}-\frac{\varepsilon X_1 z_a}{2}\right)} e^{\frac{jk_0}{2}\left(\frac{z_1'^2}{X'_1}-\frac{\varepsilon X'_1 z'_1}{2}\right)} dx_1 dS_a.\end{aligned} \tag{57}$$

2) Second Order:

$$\begin{aligned}\Psi^{(2)}_{\text{sca,flat}} \approx 8jk_0^3 &\iiint \psi^a_{\text{inc}}(\boldsymbol{r}_a) f_1 f_2 f'_2 \cot\theta_1 \\ &\times \cot\theta_2 e^{\frac{jk_0}{2}\left(\frac{z_a^2}{X_1}-\frac{\varepsilon X_1 z_a}{2}\right)} \\ &\times e^{\frac{jk_0}{2}\left(\frac{z_2'^2}{X'_2}-\frac{\varepsilon X'_2 z'_2}{2}\right)} dx_2 dx_1 dS_a.\end{aligned} \tag{58}$$

3) mth Order:

$$\begin{aligned}\Psi^{(m)}_{\text{sca,flat}} \approx (-1)^m(-2jk_0)^{m+1} &\int \cdots \int \psi^a_{\text{inc}}(\boldsymbol{r}_a) \\ &\times \prod_{k=1}^{m} f_k \cot\theta_k f'_m e^{\frac{jk_0}{2}\left(\frac{z_a^2}{X_1}-\frac{\varepsilon X_1 z_a}{2}\right)} \\ &\times e^{\frac{jk_0}{2}\left(\frac{z_m'^2}{X'_m}-\frac{\varepsilon X'_m z'_m}{2}\right)} dx_m \cdots dS_a.\end{aligned} \tag{59}$$

TABLE I
SIMULATION PARAMETERS

Duct height h [m]	50
Duct parameter ε [m^{-1}]	10^{-4}
Wavelength λ_0 [m]	0.1
Surface length L [m]	3600
Incidence angle θ_{inc} [°]	89
Vertical footprint g_z [m]	2
Antenna centre $z_{a,0}$ [m]	10
Antenna heights z_a [m]	[7;13]

V. NUMERICAL RESULTS

In this section, the coherent surface currents and the coherent scattered field are calculated using the expressions obtained in the previous sections. Furthermore, the proposed method is analyzed by comparison with a rigorous method whose advantages will be introduced in the next section.

The transmitting antenna is described in [14]. In addition, the simulation parameters are listed in Table I. The surface is considered PC ($\epsilon_{r_3} = -\infty$) for both polarizations.

A. BIE/SDIM Method

Boundary integral equation (BIE)/SDIM method was proposed in [9]. It is a rigorous method based on MoM [18], [19] and accelerated by the multilevel SDIM combined with the ACA.

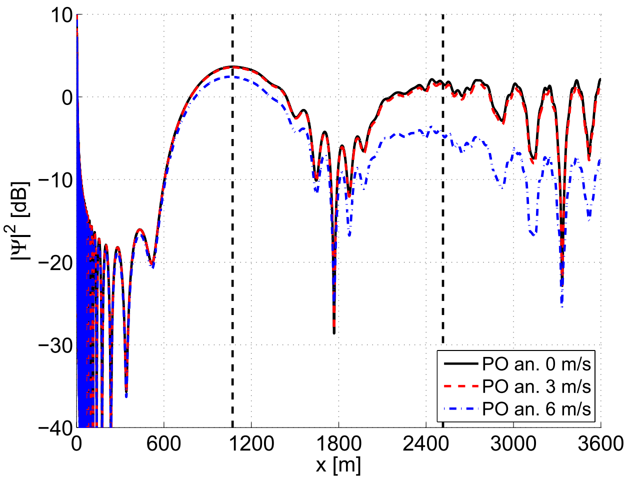

Fig. 2. Coherent current (TE polarization) on the flat and rough surfaces with respect to the horizontal distance from the transmitter for different wind speeds u_{10}. The vertical dashed lines indicate the location of the first and second rebounds predicted by a ray approach.

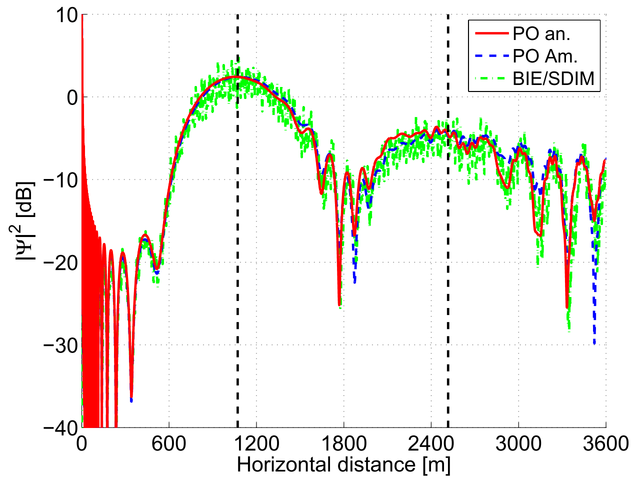

Fig. 3. Coherent current (TE polarization) on the rough surface (u_{10} = 6 m/s) with respect to the horizontal distance from the transmitter obtained by the PO and the BIE/SDIM method.

To further decrease the memory requirement, the SDIM method is extended to two levels. This means that, for each subdomain, the SDIM method is applied for the calculation of $\bar{\boldsymbol{Z}}_{i,i}^{-1}\boldsymbol{v}$. In addition, to reduce the number of iterations for K_{SDIM}, two consecutive subdomains are overlapped of about some dozens of samples ($M_{\text{Overlapping}}$), to decrease the contribution of the edge diffraction coming from the finiteness of the subdomain surfaces. Then, the memory requirement becomes $\mathcal{O}(P_1 P_2 M_2^2)$, where P_1 and P_2 are the numbers of blocks of the subdomains of levels 1 and 2, respectively, and M_2 is the number of samples on each subdomain surface of level 2 ($N = P_1 P_2 M_2$). In addition, the complexity is $\mathcal{O}(P_1 P_2 M_2^3)$.

Typically, for the results presented in Fig. 3, for a threshold $\epsilon_{\text{SDIM},1} = 10^{-2}$, $\epsilon_{\text{SDIM},2} = 10^{-3}$, $\epsilon_{\text{ACA},1} = \epsilon_{\text{ACA},2} = 10^{-3}$, $P_1 = 10 = P_2 = 10$ ($M_2 = 2880$), $M_{\text{Overlapping},1} = 10$, and $M_{\text{Overlapping},2} = 20$, we obtain $K_{\text{SDIM},1} = 7$, $K_{\text{SDIM},2} = 10$, and compression ratio $\tau_{\text{ACA},1} = 0.999$ and $\tau_{\text{ACA},2} = 0.994$, which shows that BIE/SDIM+ACA level 2 is very efficient.

This method has been validated from the MoM-based BIE/forward–backward [11] on smaller problems ($N = 48\,000$).

In the next section, PO is compared with BIE/SDIM. First, we give the results computed for TE polarization.

B. TE Polarization

Fig. 2 plots the square of coherent current modulus $|\Psi|^2$ on the 3.6-km-long surface with respect to the horizontal distance x from the source antenna on the sea surface. The analytical PO method is used to compute the coherent surface currents for two different wind speeds. The vertical dashed lines give the positions of the surface currents maxima of the first two rebounds predicted by the ray approach of the geometrical optics approximation. We observe that the obtained curves for a flat and a slightly rough surface (u_{10} = 3 m/s) are nearly the same. The current attenuation caused by the surface roughness predicted by the Ament model is relatively imperceptible (0.075 and 0.373 dB, for the first- and second-order maxima, respectively). The obtained attenuation for the wind speed of u_{10} = 6 m/s, predicted by PO, equals 1.23 and 6.15 dB for the first and second rebound maxima, respectively. Therefore, in the further comparisons to follow, we discuss only the rough surface generated by the wind speed u_{10} = 6 m/s.

In Fig. 3, the square of coherent current on the rough surface calculated by the PO method for TE polarization is compared with the one obtained by the rigorous BIE/SDIM method. The red solid line (label PO an.) represents the result computed using the completely analytical expression given by (30), and the blue dashed one (label PO Am.) shows the result with the constant reflection angle approximation from (33). A very good agreement between the results of the two methods is observed. Both PO methods show the current maxima and minima positions in agreement with those of the rigorous method.

Fig. 4 presents the total coherent power modulus above the rough surface with respect to the height z for the given horizontal distances from the transmitting antenna (60, 1800, and 3600 m). The total coherent field is defined as the sum of the incident and coherent scattered fields. The first chosen abscissa point depicts a case where the incident field is prevailing (close to the source), and the two others represent the predominant scattered field after the first and second rebounds. The analytical PO method, including the constant angle approximation [see (55)], is in agreement with the benchmark method. The slight differences that exist near the surface are due to the more rigorous Green function definition for BIE/SDIM. They can be corrected by applying the near-field correction on the Green function.

In Fig. 5, the total coherent power modulus calculated by the PO method is compared with the results obtained by the BIE/SDIM with respect to the horizontal distance x from the source for the given heights above the rough sea

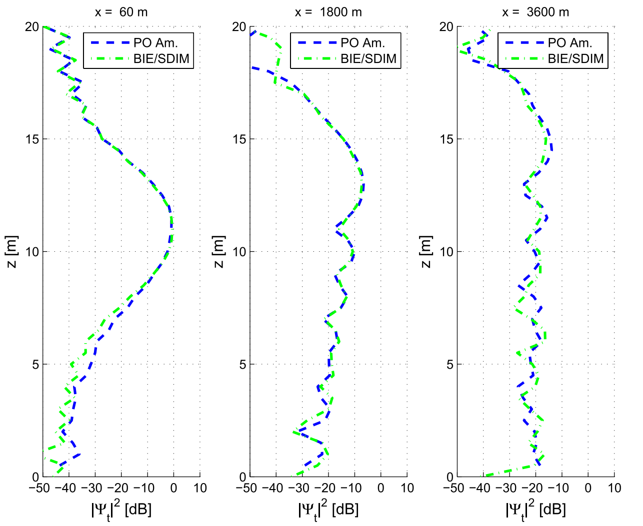

Fig. 4. Total coherent power modulus (TE polarization) above the rough sea surface ($u_{10} = 6$ m/s) with respect to the height z for given abscissas x (60, 1800, and 3600 m).

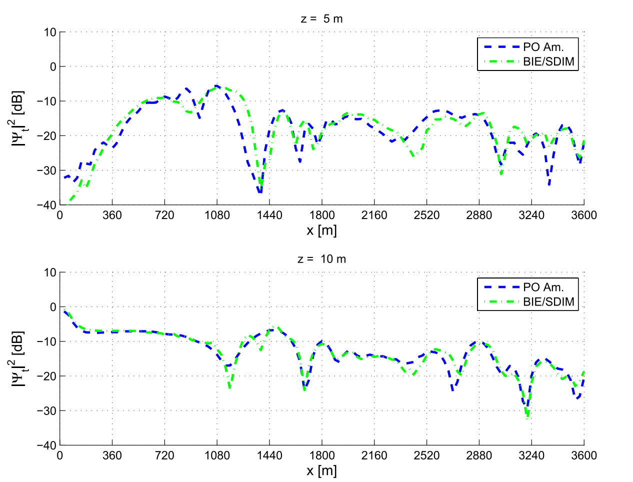

Fig. 5. Total coherent power moduli (TE polarization) above the rough sea surface ($u_{10} = 6$ m/s) with respect to the horizontal distance for given heights z (5 and 10 m).

surface (5 and 10 m). The plotted results show a good agreement. In conclusion, the PO method predicts the coherent surface current and field levels very well for TE polarization.

C. TM Polarization

Fig. 6 displays the coherent surface currents modulus versus the horizontal distance from the source obtained by the PO and the BIE/SDIM. The predictions of the maxima positions (first and second rebounds) are in agreement with those obtained by the BIE-SDIM. However, we observe a discrepancy between the two methods of around 9 dB for the first order and 18 dB for the second order. Thus, the coherent surface currents cannot be properly predicted by the PO method and the Ament model in the case of TM polarization. The same disagreement can be observed when the total coherent field is compared in Fig. 7. It is important to note that the obtained results in the case of the flat surface matched very well.

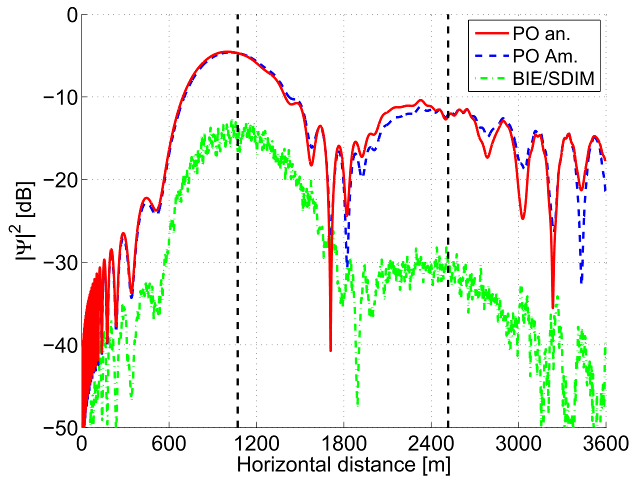

Fig. 6. Same as Fig. 3, but for TM polarization.

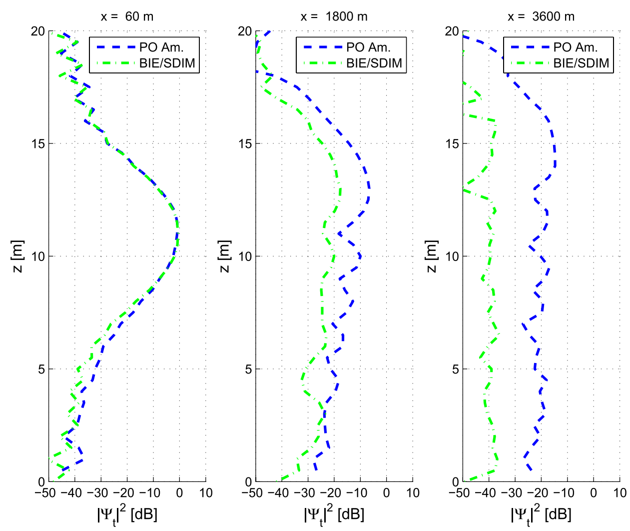

Fig. 7. Same as Fig. 4, but for TM polarization.

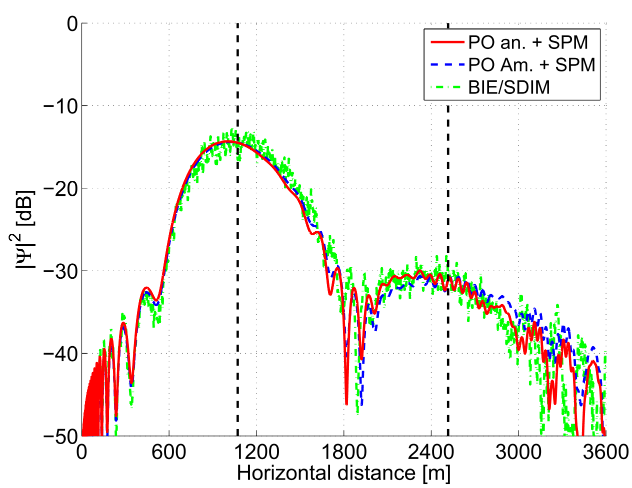

Fig. 8. Same as Fig. 3, but for TM polarization and PO method corrected by SPM.

Thus, the discrepancy is due to the surface roughness. In order to resolve this issue, a possible correction that consists in including the shadowing effect [6] is examined. First of all, the shadowing influences both polarizations, and therefore it

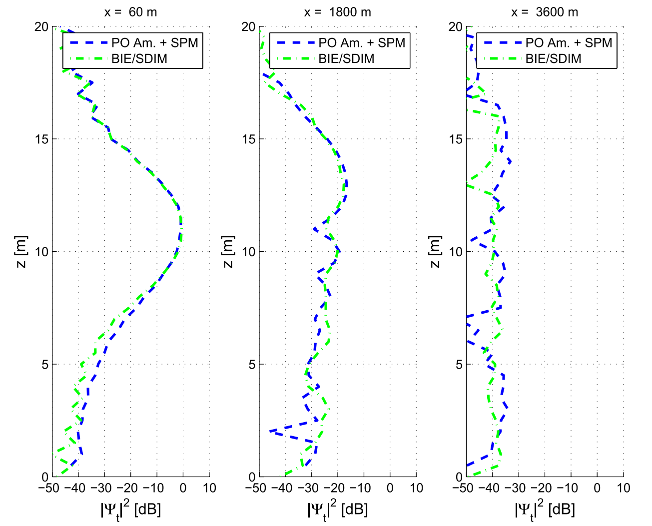

Fig. 9. Same as Fig. 4, but for TM polarization and PO method corrected by SPM.

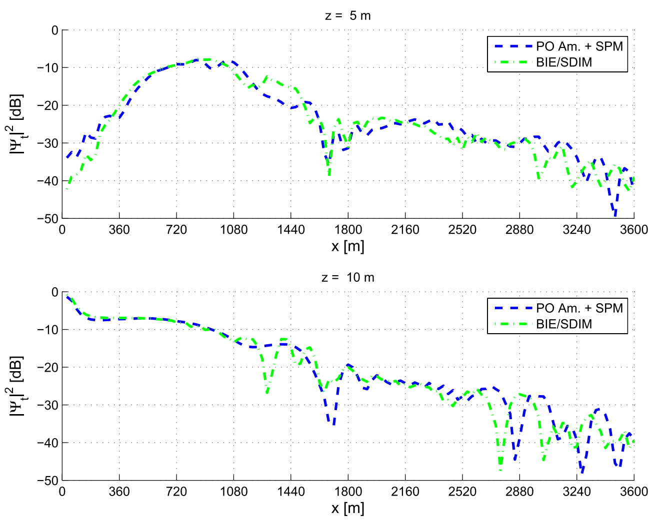

Fig. 10. Same as Fig. 5, but for TM polarization and PO method corrected by SPM.

cannot explain such a discrepancy for only one polarization. Thus, after obtaining the simulation results, this solution is dismissed. It is important to note that for TM polarization and for low-grazing angles, a phenomenon, which is similar to the Brewster-angle effect [20]–[23], occurs even for PC surfaces. This pseudo-Brewster-angle-like phenomenon is characterized by a decrease of the scattered field and it is equally observed for the slightly rough surface. It is studied within the small perturbation method (SPM), which is valid for the small-scale roughness. These studies show that the reflection coefficient changes for low-grazing angles even for a PC surface. This property is caused by the dependence of the effective impedance on the surface on the reflection angles. The necessary mathematical relations are given in Appendix C. First, we can calculate the central reflection angle from (17) obtaining $\theta_1 \approx 87.93°$. For TE polarization, from (C1), the reflection coefficient is still approximately equal to $\mathcal{R} = -1$, and the final coherent currents and field results do not change. On the other hand, for TM polarization, from (C2), the reflection coefficient significantly changed. Its calculated value is $\mathcal{R} \approx -0.401 + j0.245$, and it can be substituted in the TM polarization derivations in order to correct the final results. After applying this step, we obtained a much better agreement between our method and the reference one as can be observed in Figs. 8–10.

VI. Conclusion

In this paper, the problems of propagation and scattering are solved by applying the PO approximation in order to determine the currents on the rough sea surface. Then, an appropriate Green function of the stratified medium (duct) with linear-square refraction index profile is used to radiate the currents from Huygens' principle, and, thus, to calculate the scattered field in the duct. Due to the refraction phenomenon, this field generates new currents on the surface, which are again evaluated by PO. This process is being iterated. Then, applying the ensemble average operator on the surface currents and scattered field, for each rebound, the coherent components are calculated. Next, they are compared with those of a flat surface, leading to the generalized Ament model for multiple rebounds and in the stratified medium. The theoretical results showed the following.

1) The Ament model is a particular case of the PO approximation at the first order.
2) The coherent components (surface currents and scattered field) are expressed from the components of a flat surface multiplied by the generalized Ament coefficient.
3) For the higher orders, the generalized Ament coefficient is defined as the product of the elementary Ament coefficient for each bound. In addition, it is multiplied by a phase correction term, resulting from the phase delay between two consecutive rebounds.

For a wind speed $u_{10} = 6$ m/s and for both polarizations, the PO coherent components (surface currents and scattered field) have been compared with those calculated by the rigorous BIE/SDIM method. For TE polarization case, we observed a very good agreement between the results. However, the results obtained for TM polarization showed a significant disagreement. Indeed, the levels calculated by BIE/SDIM were much lower than the ones obtained by the PO and, therefore, the Ament model. The results showed a behavior similar to the Brewster-angle phenomenon, which is common for finitely conducting surfaces. This problem is solved using the SPM in order to calculate the new reflection coefficients. Thus, the new results show a good agreement with the reference method.

Finally, the use of the generalized Ament model avoids applying a Monte Carlo procedure, which is a costly operation.

Appendix A
Second-Order Coherent Surface Current

From (11), (22) becomes

$$\Psi_{\text{coh}}^{(2)} = -8jk_0 \iint \psi_{\text{inc}}^a(\boldsymbol{r}_a)\langle f(X_1)s(X_1, z_a, \zeta_1) \times \partial_n[f(X_2)s(X_2, \zeta_1, \zeta_2)]\rangle dx_1 dS_a \tag{A1}$$

where $X_1 = |x_a - x_1|$ and $X_2 = |x_1 - x_2|$ are the horizontal distances between the transmitter and the first rebound, respectively. Thus, it is necessary to calculate the ensemble average of the last equation.

Knowing that $s_1 = s(X_1, z_a, \zeta_1)$ and $s_2 = s(X_2, \zeta_1, \zeta_2)$ are random variables, and that $f_1 = f(X_1)$ and $f_2 = f(X_2)$ are deterministic functions, both given by (11), the ensemble average in (A1), denoted by M_2, is

$$\begin{aligned} M_2 &= \langle f_1 s_1 \partial_n (f_2 s_2)\rangle \\ &= \langle f_1 s_1 [\partial_{\zeta_1}(f_2 s_2) - \gamma_1 \partial_{x_1}(f_2 s_2)]\rangle \\ &= f_1 \langle f_2 s_1 \partial_{\zeta_1} s_2 - \gamma_1 s_1 (f_2 \partial_{x_1} s_2 + s_2 \partial_{x_1} f_2)\rangle. \end{aligned} \tag{A2}$$

This requires the calculation of the ensemble averages $\langle s_1 s_2\rangle$ and $\langle \gamma_1 s_1 s_2\rangle$, where s_1 and s_2 are given by $s(\zeta_1) = \exp(-a_{1,0}\zeta_1^2 + 2b_{1,0}\zeta_1 + c_{1,0})$ and $s(\zeta_2) = \exp(-a_{2,0}\zeta_2^2 + 2b_{2,0}\zeta_2 + c_{2,0})$, γ_1 is the surface slope $\partial_{x_1}\zeta_1$, ζ_1 is the surface height at the first rebound, and ζ_2 is the surface height at the second rebound. The random variables ζ_1 and γ_1 defined at the same point are assumed to be Gaussian and statistically independent. We can show that $\langle \gamma_1 \zeta_1\rangle = -W'_\zeta(0)$, where W_ζ is the surface height autocorrelation function [$W_\zeta(0) = \sigma_\zeta^2$] and W'_ζ its derivative with respect to x. Since W is an even function, we have $W'(0) = 0$, which implies that $\langle \gamma_1 \zeta_1\rangle = 0$. Assuming that the correlation between the random variables ζ_2 and γ_1 is negligible, this implies that $\langle \gamma_1 s_1 s_2\rangle = 0$ since $\langle \gamma_1\rangle = 0$. Thus, (A2) becomes

$$M_2 = f_1 f_2 \langle s_1 \partial_{\zeta_1} s_2\rangle. \tag{A3}$$

From the last equation, the ensemble average $\langle s_1 s_2\rangle = \left\langle e^{u(\zeta_1,\zeta_2)}\right\rangle$ must be derived, where $u(\zeta_1,\zeta_2) = -a_1\zeta_1^2 - a_2\zeta_2^2 + 2b_{12}\zeta_1\zeta_2 + 2b_1\zeta_1 + 2b_2\zeta_2 + c$, in which

$$\begin{cases} a_1 = -\dfrac{jk_0}{2}\left(\dfrac{1}{X_1} + \dfrac{1}{X_2}\right) \\ a_2 = -\dfrac{jk_0}{2X_2} \\ b_1 = -\dfrac{jk_0}{2}\left(\cot\theta_1 + \dfrac{\varepsilon X_2}{4}\right) \\ b_2 = -\dfrac{jk_0}{2}\dfrac{\varepsilon X_2}{4} \\ b_{12} = -\dfrac{jk_0}{2X_2} = a_2 \\ c = \dfrac{jk_0}{2}\left(\dfrac{z_a^2}{X_1} - \dfrac{\varepsilon X_1 z_a}{2}\right). \end{cases} \tag{A4}$$

Therefore

$$\begin{aligned} \langle e^u\rangle &= \int_{-\infty}^{+\infty}\int_{-\infty}^{+\infty} e^{u(\zeta_1,\zeta_2)} p_\zeta(\zeta_1,\zeta_2)\, d\zeta_1 d\zeta_2 \\ &= \int_{-\infty}^{+\infty}\int_{-\infty}^{+\infty} \frac{d\zeta_1 d\zeta_2}{2\pi\sqrt{\sigma_\zeta^4 - W_\zeta^2}} \\ &\quad \times e^{-\alpha_1\zeta_1^2 - \alpha_2\zeta_2^2 + 2\beta_{12}\zeta_1\zeta_2 + 2b_1\zeta_1 + 2b_2\zeta_2 + c} \end{aligned} \tag{A5}$$

where

$$\begin{cases} \alpha_1 = a_1 + \dfrac{\sigma_\zeta^2}{2\left(\sigma_\zeta^4 - W_\zeta^2\right)} \qquad \alpha_2 = a_2 + \dfrac{\sigma_\zeta^2}{2\left(\sigma_\zeta^4 - W_\zeta^2\right)} \\ \beta_{12} = b_{12} + \dfrac{W_\zeta}{2\left(\sigma_\zeta^4 - W_\zeta^2\right)} \end{cases} \tag{A6}$$

and $p_\zeta(\zeta_1,\zeta_2)$ is the surface height joint probability density function of two arbitrary surface points separated by a horizontal distance $X_2 = |x_1 - x_2|$. Moreover, $W_\zeta = W_\zeta(X_2)$ is the surface height autocorrelation function and $\sigma_\zeta^2 = W_\zeta(0)$ is the height variance.

Introducing the variable transformations $v_1 = \sqrt{\alpha_1}\zeta_1 - b_1/\sqrt{\alpha_1}$ and $v_2 = \sqrt{\alpha_2}\zeta_2 - b_2/\sqrt{\alpha_2}$, we have

$$\begin{aligned} \langle e^u\rangle &= \frac{1}{2\pi\sqrt{\alpha_1\alpha_2}\sqrt{\sigma_\zeta^4 - W_\zeta^2}} e^{c + \frac{\alpha_1 b_2^2 + \alpha_2 b_1^2 + 2\beta_{12} b_1 b_2}{\alpha_1\alpha_2}} \\ &\quad \times \int_{-\infty}^{+\infty}\int_{-\infty}^{+\infty} e^{-v_1^2 - v_2^2 + \frac{2\beta_{12}}{\sqrt{\alpha_1\alpha_2}}\left(v_1 v_2 + \frac{v_1 b_2}{\sqrt{\alpha_2}} + \frac{v_2 b_1}{\sqrt{\alpha_1}}\right)} dv_1 dv_2. \end{aligned} \tag{A7}$$

From a ray approach, in a medium with a linear-square refraction index profile, the equation of the ray trajectory of each rebound is a parabola. Thus, it is easy to show that the distance between two consecutive rebounds is $d = 4(\cot\theta_{\text{inc}}^2 + \varepsilon z_a)^{1/2}/\varepsilon$ [11], where z_a is the transmitter height, θ_{inc} is the transmitter incidence angle, and ε is the duct parameter. For $z_a = 10$ m, $\theta_{\text{inc}} = 89°$, and $\varepsilon = 10^{-4}$, the distance $d \approx 1445$ m, which is much greater than the surface height autocorrelation length. Then, the correlation between ζ_1 and ζ_2 can be neglected, leading to $W_\zeta \approx 0$. In addition, since $\sigma_\zeta \ll (X_1/k_0)^{1/2}$ ($|u_\zeta| \approx 1$) and $\sigma_\zeta \ll (X_2/k_0)^{1/2}$, $\alpha_1 \approx \alpha_2 \approx 1/(2\sigma_\zeta^2)$ and $|\beta_{12}/(\alpha_1\alpha_2)^{1/2}| \approx |b_{12}/\alpha_1| \ll 1$. Then, the exponential term in (A7) can be approximated as $e^{-v_1^2 - v_2^2}$ and the double integration over v_1 and v_2 reduces to π. As a conclusion

$$\begin{aligned} \langle e^u\rangle &\approx e^{c + \frac{b_1^2}{\alpha_1} + \frac{b_2^2}{\alpha_2} + \frac{2\beta_{12} b_1 b_2}{\alpha_1\alpha_2}} \\ &\approx e^{c + 2\sigma_\zeta^2(b_1^2 + b_2^2) + 8\sigma_\zeta^4 \beta_{12} b_1 b_2}. \end{aligned} \tag{A8}$$

Substituting (A4) into (A8), the ensemble average becomes

$$\begin{aligned} \langle e^u\rangle &\approx e^{\frac{jk_0}{2}\left(\frac{z_a^2}{X_1} - \frac{\varepsilon X_1 z_a}{2}\right)} \\ &\quad \times e^{-\frac{k_0{}^2\sigma_z^2}{2}((\cot\theta_1 + \cot\theta_2)^2 + \cot^2\theta_2)} \\ &\quad \times e^{\frac{jk_0^3\sigma_z^4\varepsilon}{4}(\cot\theta_1 + \cot\theta_2)} \end{aligned} \tag{A9}$$

where θ_2 is the incidence angle of the second rebound from the surface defined with respect to the vertical plane and

$$\cot\theta_2 = \frac{\varepsilon X_2}{4} \tag{A10}$$

obtained by the ray approach.

If the analytical integrations over v_1 and v_2 are made without any approximation, we show that

$$\langle e^u\rangle = \text{(A8)} \times e^{\frac{\beta_{12}^2}{\alpha_1^2\alpha_2^2}\left(2\beta_{12} b_1 b_2 + \alpha_1 b_2^2 + \alpha_2 b_1^2\right)} \tag{A11}$$

where $|\beta_{12}/(\alpha_1\alpha_2)^{1/2}| \ll 1$.

In addition, from (A3), we have

$$M_2 = jk_0 f_1 f_2 \left\langle \left(\frac{\zeta_1}{X_2} - \frac{\zeta_2}{X_2} - \frac{\varepsilon X_2}{4}\right) e^u \right\rangle. \tag{A12}$$

Therefore, we must derive $\langle \zeta_1 e^u \rangle$ and $\langle \zeta_2 e^u \rangle$. For $\langle \zeta_1 e^u \rangle$, we have

$$\langle \zeta_1 e^u \rangle = \frac{1}{2}\frac{\partial}{\partial b_1}\langle e^u \rangle \approx \frac{1}{\alpha_1}\left(b_1 + b_2\frac{\beta_{12}}{\alpha_2}\right)\langle e^u \rangle \approx \frac{b_1}{\alpha_1}\langle e^u \rangle \tag{A13}$$

because $|\beta_{12}/\alpha_2| \approx |2\sigma_\zeta^2 a_2| \ll 1$. Using the same way, $\langle \zeta_2 e^u \rangle \approx (b_2/\alpha_2)\langle e^u \rangle$.

Finally, from (A12) and (A13), the ensemble average is

$$M_2 \approx -jk_0 f_1 f_2 \cot\theta_2 \left[1 - \frac{jk_0\sigma_\zeta^2}{X_1}\frac{\cot\theta_1}{\cot\theta_2}\right]\langle e^u \rangle \approx -jk_0 f_1 f_2 \cot\theta_2 \langle e^u \rangle \tag{A14}$$

since $\sigma_\zeta \ll (X_1/k_0)^{1/2}$.

From (A1), (A9), and (A14), assuming that the points of consecutive rebounds, $\boldsymbol{r}_1$ and $\boldsymbol{r}_2$, are uncorrelated, the second-order coherent surface current is then

$$\Psi_{\mathrm{coh}}^{(2)} = -8k_0^2 \int_{S_a}\int_{x_1} \psi_{\mathrm{inc}}^a(\boldsymbol{r}_a) f_1 f_2 \cot\theta_2 e^{\frac{jk_0}{2}\left(\frac{z_a^2}{X_1} - \frac{\varepsilon X_1 z_a}{2}\right)} \times e^{-(R_{a,1}+R_{a,2})^2 - R_{a,2}^2} e^{\frac{jk_0^2\sigma_\zeta^3\varepsilon}{2\sqrt{2}}(R_{a,1}+R_{a,2})} dx_1 dS_a \tag{A15}$$

where $R_{a,1}$ and $R_{a,2}$ correspond to the Rayleigh roughness parameters of the Ament model divided by $\sqrt{2}$, defined by (21), and

$$R_{a,2} = \frac{k_0\sigma_\zeta \cot\theta_2}{\sqrt{2}} \tag{A16}$$

respectively.

Appendix B
Coherent Surface Current of the mth Order

In order to obtain the generalized analytical expression of the coherent surface current of the mth order ($m \geq 2$), it is necessary to compute the ensemble average M_m defined as

$$M_m = \langle g(\boldsymbol{r}_a, \boldsymbol{r}_1)\partial_n g(\boldsymbol{r}_1, \boldsymbol{r}_2)\ldots\partial_n g(\boldsymbol{r}_{m-1}, \boldsymbol{r}_m)\rangle = \left\langle f_1 s_1 \prod_{i=2}^{m}(-\gamma_{i-1}\partial_{x_{i-1}} g_i + \partial_{\zeta_{i-1}} g_i)\right\rangle \tag{B1}$$

where

$$g_i = g(\boldsymbol{r}_{i-1}, \boldsymbol{r}_i) = f_i s_i \tag{B2}$$

and

$$s_i = -a_{i,0}\zeta_i^2 + 2b_{i,0}\zeta_i + c_{i,0}. \tag{B3}$$

The parameters $a_{1,0}$, $b_{1,0}$, and $c_{1,0}$ are given by (14), and the parameters $a_{i,0}$, $b_{i,0}$, and $c_{i,0}$ are defined, for $i \geq 2$, as

$$\begin{cases} a_{i,0} = -\dfrac{jk_0}{2X_i} \\ b_{i,0} = -\dfrac{jk_0}{2}\left(\dfrac{\zeta_{i-1}}{X_i} + \dfrac{\varepsilon X_i}{4}\right) \\ c_{i,0} = \dfrac{jk_0}{2}\left(\dfrac{\zeta_{i-1}^2}{X_i} + \dfrac{\varepsilon X_i \zeta_{i-1}}{2}\right). \end{cases} \tag{B4}$$

Assuming that $\langle \gamma_i \zeta_i \rangle = W_\zeta' = 0$ for all W_ζ, we have $\langle \gamma_i f(\zeta_i)\rangle = 0, \forall f$. In addition, the correlation between the random variables (ζ_i, γ_i) and (ζ_j, γ_j) is assumed to be negligible, leading to $\langle \gamma_{i,j} f(\zeta_i, \zeta_j)\rangle = 0, \forall f$. Then, the ensemble average can be written as

$$M_m \approx f_1 \left\langle s_1 \prod_{i=2}^{m} \partial_{\zeta_i} g_i \right\rangle. \tag{B5}$$

Therefore, the ensemble average $e^{u(\zeta_1,\ldots\zeta_m)}$ must be derived, where

$$e^u = \prod_{i=1}^{m} s_i \tag{B6}$$

leading to

$$u = -a_1\zeta_1^2 - \cdots - a_m\zeta_m^2 + 2b_{12}\zeta_1\zeta_2 + \cdots + 2b_{m-1,m}\zeta_{m-1}\zeta_m + 2b_1 z_1 + \cdots + 2b_m z_m + c \tag{B7}$$

with

$$\begin{cases} a_1 = -\dfrac{jk_0}{2}\left(\dfrac{1}{X_1} + \dfrac{1}{X_2}\right) \\ a_{i,i\neq m} = -\dfrac{jk_0}{2}\left(\dfrac{1}{X_{i+1}} + \dfrac{1}{X_i}\right) \\ a_m = -\dfrac{jk_0}{2X_m} \\ b_{i-1i} = -\dfrac{jk_0}{2X_i} \\ b_{i,i\neq m} = -\dfrac{jk_0}{2}(\cot\theta_i + \cot\theta_{i+1}) \\ b_m = -\dfrac{jk_0}{2}\cot\theta_m \\ c = \dfrac{jk_0}{2}\left(\dfrac{z_a^2}{X_1} - \dfrac{\varepsilon X_1 z_a}{2}\right). \end{cases} \tag{B8}$$

Analogously to the calculation in Appendix A, by neglecting the correlation between any ζ_i and ζ_j, for $i \neq j$, we obtain

$$\langle e^u \rangle \approx e^{c + \sum_{i=1}^{m}\frac{b_i^2}{\alpha_i} + \sum_{j=2}^{m}\frac{2\beta_{j-1,j}b_{j-1,}b_j}{\alpha_{j-1}\alpha_j}} \tag{B9}$$

with

$$\begin{cases} \alpha_i \approx a_i + \dfrac{1}{2\sigma_\zeta^2} \\ \beta_{j-1,j} \approx b_{j-1,j}. \end{cases} \tag{B10}$$

Substituting (B8) into (B9) and introducing the local incidence angle of the ith rebound, obtained by the ray approach as

$$\cot\theta_i = \frac{\varepsilon X_i}{4}, \quad i \geq 2 \tag{B11}$$

we find the ensemble average of the mth order, $m \geq 2$, as follows:

$$\langle e^u \rangle = e^{\frac{jk_0}{2}\left(\frac{z_a^2}{X_1} - \frac{\varepsilon X_1 z_a}{2}\right)} \times e^{\sum_{i=1}^{m-1} -\frac{k_0^2\sigma_\zeta^2}{2}(\cot\theta_i + \cot\theta_{i+1})^2 - \frac{k_0^2\sigma_\zeta^2}{2}\cot\theta_m^2} \times e^{\sum_{j=1}^{m-1}\frac{jk_0^3\sigma_\zeta^4\varepsilon}{4\cot\theta_j}(\cot\theta_{j-1} + \cot\theta_j)(\cot\theta_j + \cot\theta_{j+1})} \times e^{\frac{jk_0^3\sigma_\zeta^4\varepsilon}{4}(\cot\theta_{m-1} + \cot\theta_m)}. \tag{B12}$$

Finally, from (B4), (B5), and (B9), we get the ensemble average of the coherent surface current of the mth order, $m \geq 2$

$$\begin{aligned} M_m &= f_1 \left\langle \prod_{k=2}^{m} jk_0 f_k \left(\frac{\zeta_{k-1}}{X_k} - \frac{\zeta_k}{X_k} - \frac{\varepsilon X_k}{4} \right) e^u \right\rangle \\ &\approx (-jk_0)^{m-1} \langle e^u \rangle \prod_{k=2}^{m} f_k \cot\theta_k. \end{aligned} \tag{B13}$$

Thus, from (29), (B12), and (B13), the coherent surface current at the mth order is

$$\begin{aligned} \Psi_{\mathrm{coh}}^{(m)} \approx\ & 2(-2jk_0)^m \int \cdots \int \psi_{\mathrm{inc}}^{a}(\boldsymbol{r}_a) f_1 \prod_{k=2}^{m} f_k \cot\theta_k \\ & \times e^{\frac{jk_0}{2}\left(\frac{z_a^2}{X_1} - \frac{\varepsilon X_1 z_a}{2}\right)} e^{-R_{a,m}^2 - \sum_{i=1}^{m-1}(R_{a,i}+R_{a,i+1})^2} \\ & \times e^{\frac{jk_0^2\sigma_\zeta^3\varepsilon}{2\sqrt{2}} \sum_{j=2}^{m-1} R_{a,j}\left(1+\frac{R_{a,j-1}}{R_{a,j}}\right)\left(1+\frac{R_{a,j+1}}{R_{a,j}}\right)} \\ & \times e^{\frac{jk_0^2\sigma_\zeta^3\varepsilon}{2\sqrt{2}}(R_{a,m-1}+R_{a,m})} dx_{m-1}\ldots dx_1 dS_a. \end{aligned} \tag{B14}$$

Appendix C
Reflection Coefficient Calculation for PC Surfaces by SPM

From [20], based on [24], the first-order reflection coefficients for Dirichlet and Neumann boundary conditions are given by

$$\mathcal{R}_{\mathrm{TE}} = \frac{k_z(\kappa) Z_{\mathrm{TE}}(\kappa) - k_0}{k_z(\kappa) Z_{\mathrm{TE}}(\kappa) + k_0} \tag{C1}$$

and

$$\mathcal{R}_{\mathrm{TM}} = \frac{k_z(\kappa) - k_0 Z_{\mathrm{TM}}(\kappa)}{k_z(\kappa) + k_0 Z_{\mathrm{TM}}(\kappa)}. \tag{C2}$$

Here wave vector is defined by $\boldsymbol{k}_0 = \kappa\hat{\boldsymbol{x}} + k_z(\kappa)\hat{\boldsymbol{z}}$, where k_0 is the wavenumber, and k_z is obtained from

$$k_z(\kappa) = \begin{cases} \sqrt{k_0^2 - \kappa^2} & \text{for } \kappa \leq k_0 \\ j\sqrt{\kappa^2 - k_0^2} & \text{for } \kappa > k_0. \end{cases} \tag{C3}$$

In addition, Z_{TE} and Z_{TM} denote the effective surface impedances of the first order. They are expressed by

$$Z_{\mathrm{TE}} = \int_{-\infty}^{+\infty} d\kappa' k_z(\kappa') \tilde{W}(\kappa - \kappa') \tag{C4}$$

and

$$Z_{\mathrm{TM}} = \int_{-\infty}^{+\infty} d\kappa' \frac{\left(k_0^2 - \kappa\kappa'\right)^2}{k_0 k_z(\kappa')} \tilde{W}(\kappa - \kappa') \tag{C5}$$

where $\tilde{W}$ is the isotropic sea spectrum. More details on these integrations are given in [20].

References

[1] W. S. Ament, "Toward a theory of reflection by a rough surface," *Proc. IRE*, vol. 41, no. 1, pp. 142–146, Jan. 1953.

[2] M. Levy, *Parabolic Equation Methods for Electromagnetic Wave Propagation* (Electromagnetic Waves Series). London, U.K.: Institution of Electrical Engineers, 2000.

[3] A. R. Miller, R. M. Brown, and E. Vegh, "New derivation for the rough-surface reflection coefficient and for the distribution of sea-wave elevations," *IEE Proc. H Microw., Opt. Antennas*, vol. 131, no. 2, pp. 114–116, Apr. 1984.

[4] D. E. Freund, N. E. Woods, H.-C. Ku, and R. S. Awadallah, "Forward radar propagation over a rough sea surface: A numerical assessment of the miller-brown approximation using a horizontally polarized 3-GHz line source," *IEEE Trans. Antennas Propag.*, vol. 54, no. 4, pp. 1292–1304, Apr. 2006.

[5] T. S. Hristov, K. D. Anderson, and C. A. Friehe, "Scattering properties of the ocean surface: The Miller–Brown–Vegh model revisited," *IEEE Trans. Antennas Propag.*, vol. 56, no. 4, pp. 1103–1109, Apr. 2008.

[6] V. Fabbro, C. Bourlier, and P. F. Combes, "Forward propagation modeling above Gaussian rough surfaces by the parabolic shadowing effect," *Prog. Electromagn. Res.*, vol. 58, pp. 243–269, 2006.

[7] N. Pinel, C. Bourlier, and J. Saillard, "Forward radar propagation over oil slicks on sea surfaces using the Ament model with shadowing effect," *Prog. Electromagn. Res.*, vol. 76, pp. 95–126, 2007.

[8] D. E. Freund, N. E. Woods, H.-C. Ku, and R. S. Awadallah, "The effects of shadowing on modelling forward radar propagation over a rough sea surface," *Waves Random Complex Media*, vol. 18, no. 3, pp. 387–408, Aug. 2008.

[9] C. Bourlier, S. Bellez, H. Li, and G. Kubické, "Sub-domain decomposition iterative method combined with ACA: An efficient technique for the scattering from a large highly conducting rough sea surface," *IEEE Trans. Antennas Propag.*, vol. 63, no. 2, pp. 659–666, Feb. 2015.

[10] T. Elfouhaily, B. Chapron, K. Katsaros, and D. Vandemark, "A unified directional spectrum for long and short wind-driven waves," *J. Geophys. Res., Oceans*, vol. 102, no. C7, pp. 15781–15796, 1997.

[11] C. Bourlier, H. Li, and N. Pinel, "Low-grazing angle propagation and scattering above the sea surface in the presence of a duct jointly solved by boundary integral equations," *IEEE Trans. Antennas Propag.*, vol. 63, no. 2, pp. 667–677, Feb. 2015.

[12] F. G. Bass and I. M. Fuks, *Wave Scattering from Statistically Rough Surfaces*. Oxford, U.K.: Pergamon, 1978.

[13] J. V. Toporkov, R. S. Awadallah, and G. S. Brown, "Issues related to the use of a Gaussian-like incident field for low-grazing-angle scattering," *J. Opt. Soc. Amer.*, vol. 16, no. 1, pp. 176–187, 1999.

[14] C. Bourlier and N. Pinel, "Spatial Green function of a constant medium overlying a duct with linear-square refractive index profile," *IEEE Trans. Antennas Propag.*, vol. 61, no. 6, pp. 3172–3181, Jun. 2013.

[15] C. Bourlier and J. Berginc, "Microwave analytical backscattering models from randomly rough anisotropic sea surface—Comparison with experimental data in C and Ku bands," *Prog. Electromagn. Res.*, vol. 37, pp. 31–78, 2002.

[16] L. M. Brekhovskikh, *Waves in Layered Media*, 2nd ed. New York, NY, USA: Academic, 1980.

[17] Y. A. Kravtsov and Y. I. Orlov, *Geometrical Optics of Inhomogeneous Media*. Berlin, Germany: Springer-Verlag, 1990.

[18] R. F. Harrington, *Field Computation by Moment Methods*. New York, NY, USA: Macmillan, 1968.

[19] L. Tsang, J. A. Kong, K.-H. Ding, and C. O. Ao, *Scattering of Electromagnetic Waves, Numerical Simulations*. New York, NY, USA: Wiley, 2001.

[20] Y. Brelet and C. Bourlier, "SPM numerical results from an effective surface impedance for a one-dimensional perfectly-conducting rough sea surface," *Prog. Electromagn. Res.*, vol. 81, pp. 413–436, 2008.

[21] A. Ishimaru, J. D. Rockway, and Y. Kuga, "Rough surface Green's function based on the first-order modified perturbation and smoothed diagram methods," *Waves Random Media*, vol. 10, no. 1, pp. 17–31, 2000.

[22] I. M. Fuks, V. I. Tatarskii, and D. E. Barrick, "Behaviour of scattering from a rough surface at small grazing angles," *Waves Random Media*, vol. 9, no. 3, pp. 295–305, 1999.

[23] D. E. Barrick, "Grazing behavior of scatter and propagation above any rough surface," *IEEE Trans. Antennas Propag.*, vol. 46, no. 1, pp. 73–83, Jan. 1998.

[24] S. Ito, "Analysis of scalar wave scattering from slightly rough random surfaces: A multiple scattering theory," *Radio Sci.*, vol. 20, no. 1, pp. 1–12, 1985.

Dušan Cvetković was born in Leskovac, Serbia, in 1986. He received the Engineering degree in telecommunications from the Faculty of Electronic Engineering, University of Niš, Niš, Serbia, in 2010, and the M.S. degree in electronic systems and the Ph.D. degree from Polytech Nantes, Université de Nantes, Nantes, France, in 2012 and 2016, respectively.

He is currently with the Institute of Electronics and Telecommunications of Rennes, Nantes. He is also a Post-Doctoral Researcher on electromagnetic wave propagation and scattering in the marine environment.

Christophe Bourlier was born in La Flèche, France, in 1971. He received the M.S. degree in electronics from the University of Rennes, Rennes, France, in 1995, and the Ph.D. degree from the Systèmes Electroniques et Informatique Laboratory, Nantes, France, in 1999.

He is currently with the Institute of Electronics and Telecommunications of Rennes, Polytech Nantes, Université de Nantes, Nantes. He is also a Researcher with the National Center for Scientific Research, Paris, France, where he is involved in electromagnetic wave scattering from rough surfaces (ocean like-surfaces) and objects for microwaves and infrared remote sensing applications and radar signatures. He has authored over 180 journal articles and conference papers.

Nicolas Pinel was born in Saint-Brieuc, France, in 1980. He received the Engineering degree and the M.S. degree in electronics and electrical engineering from Polytech Nantes, Université de Nantes, Nantes, France, in 2003, and the Ph.D. degree from the Université de Nantes, in 2006.

He was with Polytech Nantes as a Contractual Assistant Professor for two years and then as a Research Engineer for five years. He has been a Research and Development Engineer with Alyotech, Rennes, France, since 2013. His current research interests include radar and optical remote sensing, scattering, and propagation, in particular, asymptotic methods of electromagnetic wave scattering from random rough surfaces and layers.